Fiber-pigtailed optical tweezer for single-atom trapping and single-photon generation

S. Garcia,[1] D. Maxein,[1] L. Hohmann,[1] J. Reichel,[1] and R. Long[1, a)]
Laboratoire Kastler Brossel, ENS, Université Pierre et Marie Curie-Paris 6, CNRS, 24 rue Lhomond, 75 005 Paris, France

(Dated: 14 October 2013)

We demonstrate a miniature, fiber-coupled optical tweezer to trap a single atom. The same fiber is used to trap a single atom and to read out its fluorescence. To obtain a low background level, the tweezer light is chopped, and we measure the influence of the chopping frequency on the atom's lifetime. We use the single atom as a single-photon source at 780 nm and measure the second-order correlation function of the emitted photons. Because of its miniature, robust, fiber-pigtailed design, this tweezer can be implemented in a broad range of experiments where single atoms are used as a resource.

Trapped single atoms are an enabling tool in quantum science and technology, and are investigated for applications from quantum information[1–5] to quantum sensing[6]. On par with single ions, they also provide the best performance among all emitters for indistinguishable, narrow-band single photons[7]. So far however, one of their major drawbacks has been the size and complexity of single-atom sources[8]. Here we demonstrate single-atom trapping and single-photon production with a simple and practical, miniature optical tweezer. The device is fiber coupled, making it robust and simplifying its integration as part of a more complex experiment. It is also cheap to build and does not require cleanroom techniques. Chopping the dipole trap completely eliminates trap-induced light shifts and broadening in the single-photon spectrum. In addition to single-photon generation, this device substantially simplifies the production of single atoms for applications in quantum information and quantum optics.

A well-established technique to trap single atoms is the use of a tightly confining far off-resonance optical trap. For a single, red-detuned beam, atoms are attracted toward the beam focus due to the dipole force. If this optical tweezer is confining enough, the "collisional blockade" effect efficiently eliminates states with more than one atom, guaranteeing that no more than one atom is present inside the trap[1]. To enter the collisional blockade regime, high numerical aperture optics are needed, making integration and scalability challenging and costly. On the other hand, it has already been demonstrated that the trapping of single atoms is possible with a single, commercially available aspheric lens, which is placed inside the vacuum chamber[9–11]. In those experiments however, the light enters and leaves the vacuum as a free-space beam, requiring macroscopic lenses and careful alignment, further compromising scalability. In contrast to these setups, our approach relies on a miniature, fiber-pigtailed device terminated with a small commercial aspheric lens and placed entirely inside the vacuum chamber. By combining this device with the technique of chopping the dipole light[12], we are able to use the same fiber for dipole light delivery and single-atom fluorescence extraction with low background.

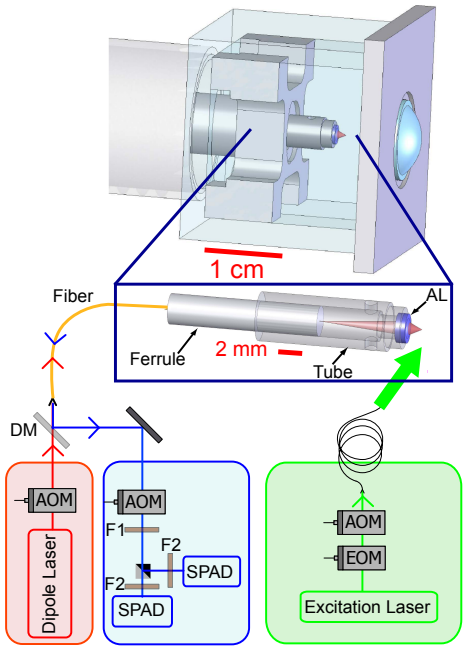

FIG. 1. The fiber-optical tweezer: the aspheric lens (AL) is glued to the end of a ceramic tube, the fiber inside a ferrule is glued inside the bore of the tube leading to a 1.4 μm waist at 1 mm from the lens. Laser setup: The dipole light and the fluorescence light are split by a dichroic mirror (DM). A custom filter (F1) and standard filters (F2) on the detection path to the single-photon avalanche diodes (SPAD) remove background dipole trap light. The excitation pulses for single photon generation are obtained by sending a continuous laser through an intensity EOM followed by an AOM.

In our prototype setup, the aspheric lens (LightPath Technologies Model 355200) is glued to the end of a machinable ceramic tube. The fiber is glued inside a ceramic ferrule, which is inserted into the bore of the ceramic tube (Fig. 1). We optimize the position of the

a)Electronic mail: long@lkb.ens.fr

ferrule inside the tube to obtain the smallest possible waist at the trapping wavelength (1.4 μm) before gluing it inside the tube. The focus is at 1 mm from the end face of the lens. We use ^{87}Rb atoms with an emission wavelength of 780 nm (D2 line) and dipole trapping light with a wavelength close to 810 nm. An inherent advantage of our design is that the trap position and the collection focus coincide very well if the dipole and fluorescence wavelength are not too far apart[13]. Along the optical axis, the two foci are distant by 2 μm (about one third of the Rayleigh range), which ensures a good collection efficiency without any further alignment. This prealigned system is placed inside a cubic, 25 mm side length, all-glass cell intended for spectroscopy (Hellma 704.000). A simple fiber feed-through[14] is sufficient to bring the light into and out of the vacuum chamber. Loading of the dipole trap is achieved by producing a cloud of laser-cooled atoms in a magneto-optical trap (MOT) at the focus of the dipole beam. For the MOT, we use three retro-reflected beams 1 mm in diameter, with two of them crossing at an angle of 20 ° to avoid clipping at the lens. The dipole light is chopped with an acousto-optical modulator (AOM), single-photons being detected while the dipole trap is off. This eliminates trap-induced light shifts as a source of spectral broadening. It also avoids the generation of 780 nm photons by anti-Stokes Raman scattering of the trapping light inside the fiber, which would obfuscate the single-atom fluorescence[15,16].

In a first experiment, we keep the MOT light always on. During the dark phase (dipole light off), we count the fluorescence photons emitted by an atom and collected via the lens and fiber. We separate the fluorescence light from the dipole light with a dichroic mirror (Semrock LPD01-785RU-25). To block background light of the dipole laser, we use a custom interference filter centered at 780 nm with a bandwidth of 0.3 nm and a transmission of about 90 %, followed by commercial interference filter (Semrock LL01-780-12.5). Additionally, we use an acousto-optical modulator to open the detection path only during the dark phase of the dipole laser, thus preventing Raman photons from the fiber pigtail from reaching a single-photon avalanche diode (SPAD). (These photons otherwise create a background during the detection window, probably due to delayed afterpulses of our SPAD[17].) The fluorescence light is then coupled into a multimode fiber and detected by the SPAD (Excelitas Technologies SPCM-AQRH-13-FC). With this setup, we observe a background rate of about 100 counts/s (dark counts and remaining Raman/afterpulse contribution) when the MOT is off, and 2100 cts/s when the MOT is on. This is low enough that in the presence of the MOT beams, we can see a high-contrast two-level fluorescence signal, jumping between photon count rates corresponding to zero or one atom inside the trap (Fig. 2(a)). We do not observe any two-atom events within our binning resolution of 10 ms, indicating that the trap operates in the blockade regime where light-assisted two-body collisions lead to a rapid loss of the two atoms. Fig. 2(b) shows

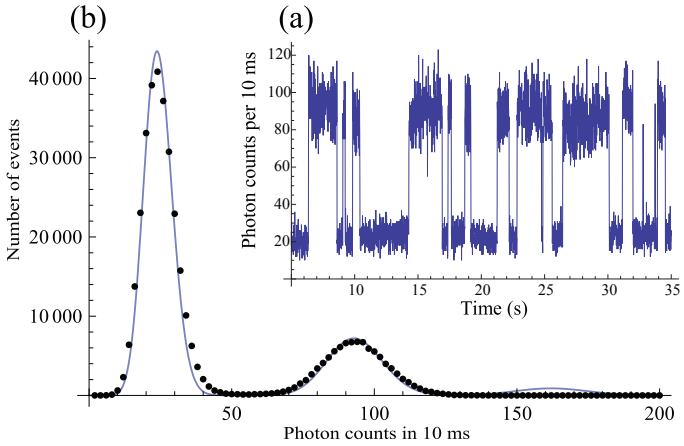

FIG. 2. **a)** Number of counted photons for 10 ms time bins showing step signal. **b)** Histogram of counted photons during 3850 s (black points) with a fit by a compound Poisson law for 0, 1 and 2 atoms peaks (solid line).

a histogram of counts recorded during 3850 s. Fitting it with a compound Poisson law underscores the complete absence of a two-atom peak, confirming the single atom trapping ability of our trap.

We have investigated the influence of the trap chopping frequency on the lifetime of the atom inside the trap in the presence of the MOT beams. With a duty cycle of 50 %, the time-averaged dipole light power is 6.9 mW, corresponding to a trap depth of 2.8 mK. To be mainly limited by background gas collisions, we work in the weak loading regime, where loss due to a second atom entering the trap is negligible. When the dipole light is on, the transverse and longitudinal trap frequencies are 167 kHz and 22 kHz, respectively. For chopping frequencies larger than the trap frequencies, we expect the atom to experience a time-averaged potential in which it can stay trapped. In Fig. 3, we observe, with linearly polarized dipole light, a lifetime of about 400 ms for frequencies above 2 MHz, limited by background gas collisions. For frequencies below 2 MHz, the lifetime decreases with the chopping frequency. Below 500 kHz, we could not detect any single-atom trapping signal. We notice that the lifetime of the atom is very sensitive to the polarisation of the dipole light and is actually improved by adding a small circular polarisation. This behavior could be due to a residual magnetic field which is compensated by an effective magnetic field generated by the circular polarisation of the light, leading to a better cooling of the atoms inside the dipole trap[18].

In the following, we use the single atoms as a single-photon source[19]. For single photon generation, it is critical to further reduce the background level. This is easily achieved by switching off the MOT light after loading the dipole trap. To obtain a single photon source, we use the following timing sequence. The chopping frequency is fixed at 2 MHz. During a loading phase, we apply the MOT lasers and the magnetic field gradient until two

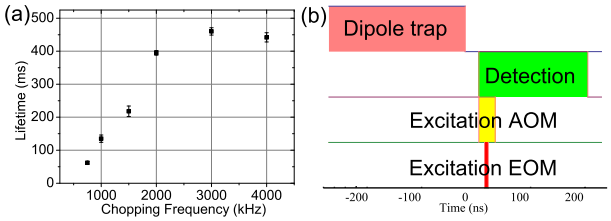

FIG. 3. **a)** Dipole trap lifetime in presence of the MOT versus chopping frequency, for linearly polarized dipole light. **b)** Timing sequence. For the data in Figs. 2 and 3(a), we chop the dipole light and the detection path. For single photon generation, we switch off the MOT and apply resonant excitation pulses by using a CW laser passing through an intensity-EOM followed by an AOM.

consecutive 10 ms integration intervals of the fluorescence counts are above a threshold which depends on the background and single-atom count rates. This loading phase has an average duration of 1 s. We then turn the MOT lasers and the magnetic gradient off, leaving the single atom inside the chopped dipole trap. A stream of single photons is produced from the trapped atom by resonantly exciting it with a π-pulse each time the dipole light is off. The excitation beam is tuned on the transition $\left|5^2\mathrm{S}_{1/2}, F=2\right\rangle \rightarrow \left|5^2\mathrm{P}_{3/2}, F'=3\right\rangle$ and aligned orthogonally to the trap axis (see Fig. 1). The pulses are generated by sending a continuous laser through an electro-optic intensity modulator (EOM, Jenoptik AM780HF). The pulse duration is set to $\tau = 3.5$ ns in order to avoid double excitation of the atom (excited state lifetime $\tau \ll 26$ ns) and excitation to other states due to Fourier-broadened linewidth ($\tau \gg 1/(2\Delta\omega) \simeq 1.9$ ns, where $\hbar\Delta\omega$ is the energy difference between the $F'=2$ and $F'=3$ excited states). As the EOM's extinction ratio of 800 is not high enough to completely avoid excitation during the off-phase, we add an AOM for additional extinction. We pulse this AOM with a duration of 30 ns (limited by the AOM response), centered on the EOM pulse. The excitation beam waist is 50 μm at the position of the dipole trap. The polarization is σ^+ relative to a 4×10^{-4} T quantization magnetic field applied in the laser propagation direction. In order to obtain a π-pulse, we adjust the peak pulse power by observing the time distribution of the photons detected by the SPAD after the pulse. This results in a peak power of about 2 mW.

During the photon generation phase, the quantification field is applied continuously and the timing sequence is as follows. After the end of every dipole light pulse (i.e., every 500 ns), labeled $t = 0$, we open the detection path and the excitation AOM at $t = 25$ ns. At $t = 45$ ns, we apply the 3.5 ns π-pulse. The atom emits a single photon during the 200 ns detection window with a calculated probability of 99.9 %. While the dipole laser is on, we also switch on a repumping laser, resonant on the transition $\left|5^2\mathrm{S}_{1/2}, F=1\right\rangle \rightarrow \left|5^2\mathrm{P}_{3/2}, F'=2\right\rangle$, to repump atoms that may have fallen into the $F = 1$ level. The duration of the photon generation phase is set to 2 ms, corresponding to 4000 excitation sequences, after which another loading phase follows. With such a short photon generation phase, the atom remains trapped at the end of this phase with high probability. This shortens the ensuing loading phase, maximizing the average single-photon flux. During the photon generation phase, the single-photon collection rate into the fiber is about 13500 photons/s, which corresponds to a collection efficiency of about 0.7 %. On average, including the loading phase, we obtain approximately 170 single photons per second out of the fiber. With the reasonable assumption that the single atom is a Fourier-transform limited source, we obtain an average spectral brightness of 28 photons/(s MHz). This is better than state-of-the-art diamond-based single-photon emitters[20] and comparable to some non-deterministic parametric down conversion sources[21,22], while keeping the advantage of atomic sources in terms of indistinguishability of the emitted photons.

To prove the single-photon characteristics of our source, we have measured the second-order intensity correlations of the light field by implementing a Hanbury-Brown and Twiss setup[23]. The results are presented in Fig. 4 without any background subtraction. The peaks at multiples of 500 ns delay are due to correlations between photons generated by different excitation pulses. Half of the relative area of the zero-delay peak, normalized to that of a 500 ns delayed peak, gives approximately the probability to emit two photons per excitation pulse[24]. We find a probability of $(4.5 \pm 0.5)\%$ without background correction. Subtracting the known contribution of SPAD dark count noise yields a $(3 \pm 0.6)\%$ probability of emitting two photons per pulse. This limit is mainly due to the fact that the atom can be excited twice during the detection window. The probability of double excitation is 2% during the pulse itself and 1% during the time where the EOM is off but the AOM still open. The latter contribution could be avoided by using two EOMs in series. We have simulated the excitation using the optical Bloch equations, taking into account the EOM and AOM pulse shapes as well as the detector dark counts. It fits the data quite well (see Fig. 4) and gives a two-photon emission probability of 3.3%, close to the experimental value.

In conclusion, we have developed a miniature fiber-pigtailed optical tweezer for single atom trapping and detection. Though in this experiment the tweezer stays fixed, it is possible in principle to move it within a vacuum chamber, providing a scanning cold single-atom probe. An advantage of this approach is the possibility to move the single atom without being limited by the transverse field of view, enabling the delivery of single atoms inside an optical cavity[6,25,26] or the probing of surfaces at very short distances[27]. Further miniaturization is possible by fabricating a lens directly on the fiber tip, reducing the volume of the tweezer by another three orders of magnitude. We have also demonstrated the use of the pigtailed tweezer as a single photon source based on a single atomic emitter. Despite its low flux, we expect this

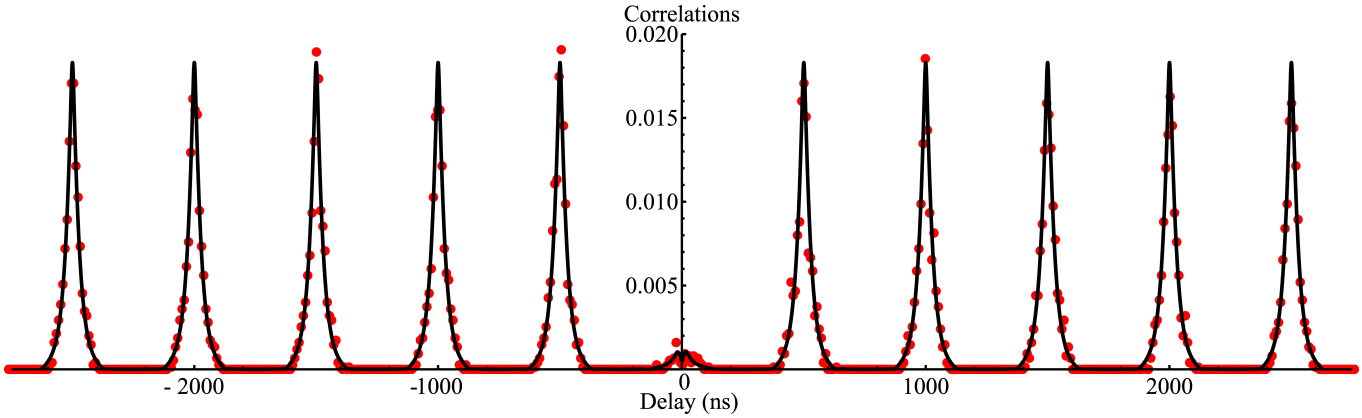

FIG. 4. Second-order intensity correlations (normalized units). Red dots are experimental data with 8 ns binning. The black curve is an optical Bloch equation simulation including experimental noise. Near-zero coincidences around zero delay are the signature of a single photon source.

source to generate single photons with excellent indistinguishability. This is due to the very good spatial mode matching between single photons which are fiber-coupled by design, and due to the fact that we excite the atoms when the dipole trap is off, so that there is no broadening induced by light shifts. These features make the fiber-pigtailed tweezer attractive for hybrid, cold atom-surface science techniques as well as for complex quantum engineering networks where single atoms are used as a resource.

ACKNOWLEDGMENTS

We acknowledge funding from Émergence-UPMC-2009 research program and from the EU STREP project QIBEC. D. M. acknowledges a post-doctoral grant from the Émergence-UPMC-2009 research program. We thank I. Saideh and M. Ammar for contributions in the early stage of the experiment.

[1] N. Schlosser, G. Reymond, I. Protsenko, and P. Grangier, Nature **411**, 1024 (2001).
[2] J. Volz, M. Weber, D. Schlenk, W. Rosenfeld, J. Vrana, K. Saucke, C. Kurtsiefer, and H. Weinfurter, Phys. Rev. Lett. **96**, 030404 (2006).
[3] T. Wilk, A. Gaëtan, C. Evellin, J. Wolters, Y. Miroshnychenko, P. Grangier, and A. Browaeys, Phys. Rev. Lett. **104**, 010502 (2010).
[4] L. Isenhower, E. Urban, X. L. Zhang, A. T. Gill, T. Henage, T. A. Johnson, T. G. Walker, and M. Saffman, Phys. Rev. Lett. **104**, 010503 (2010).
[5] J. Hofmann, M. Krug, N. Ortegel, L. Grard, M. Weber, W. Rosenfeld, and H. Weinfurter, Science **337**, 72 (2012).
[6] J. D. Thompson, T. G. Tiecke, N. P. de Leon, J. Feist, A. V. Akimov, M. Gullans, A. S. Zibrov, V. Vuletic, and M. D. Lukin, Science **340**, 1202 (2013).
[7] M. D. Eisaman, J. Fan, A. Migdall, and S. V. Polyakov, Rev. Sci. Instrum. **82**, 071101 (2011).
[8] B. Lounis and M. Orrit, Rep. Prog. Phys. **68**, 1129 (2005).
[9] Y. R. P. Sortais, H. Marion, C. Tuchendler, A. M. Lance, M. Lamare, P. Fournet, C. Armellin, R. Mercier, G. Messin, A. Browaeys, and P. Grangier, Phys. Rev. A **75**, 013406 (2007).
[10] M. K. Tey, Z. Chen, S. A. Aljunid, B. Chng, F. Huber, G. Maslennikov, and C. Kurtsiefer, Nat. Physics **4**, 924 (2008).
[11] T. Grünzweig, A. Hilliard, M. McGovern, and M. F. Andersen, Nat. Physics **6**, 951 (2010).
[12] S. Chu, J. E. Bjorkholm, A. Ashkin, and A. Cable, Phys. Rev. Lett. **57**, 314 (1986).
[13] A. Takamizawa, T. Steinmetz, R. Delhuille, T. W. Hänsch, and J. Reichel, Opt. Express **14**, 10976 (2006).
[14] E. R. I. Abraham and E. A. Cornell, Appl. Opt. **37**, 1762 (1998).
[15] M. Farahani and T. Gogolla, J. Lightwave Technol. **17**, 1379 (1999).
[16] K. Suh and C. Lee, Opt. Lett. **33**, 1845 (2008).
[17] J. Enderlein and I. Gregor, Rev. Sci. Instrum. **76**, 033102 (2005).
[18] B. S. Mathur, H. Tang, and W. Happer, Phys. Rev. **171**, 11 (1968).
[19] B. Darquié, M. P. A. Jones, J. Dingjan, J. Beugnon, S. Bergamini, Y. Sortais, G. Messin, A. Browaeys, and P. Grangier, Science **309**, 454 (2005).
[20] I. Aharonovich, S. Castelletto, D. Simpson, C.-H. Su, A. Greentree, and S. Prawer, Rep. Prog. Phys. **74**, 076501 (2011).
[21] A. Haase, N. Piro, J. Eschner, and M. W. Mitchell, Opt. Lett. **34**, 55 (2009).
[22] J. Fekete, D. Rieländer, M. Cristiani, and H. de Riedmatten, Phys. Rev. Lett. **110**, 220502 (2013).
[23] R. Hanbury Brown and R. Q. Twiss, Nature **177**, 27 (1956).
[24] J. McKeever, A. Boca, A. D. Boozer, R. Miller, J. R. Buck, A. Kuzmich, and H. J. Kimble, Science **303**, 1992 (2004).
[25] D. E. Chang, J. D. Thompson, H. Park, V. Vuletić, A. S. Zibrov, P. Zoller, and M. D. Lukin, Phys. Rev. Lett. **103**, 123004 (2009).
[26] D. J. Alton, N. P. Stern, T. Aoki, H. Lee, E. Ostby, K. J. Vahala, and H. J. Kimble, Nat. Physics **7**, 159 (2011).
[27] L. P. Parazzoli, A. M. Hankin, and G. W. Biedermann, Phys. Rev. Lett. **109**, 230401 (2012).